

Icebreaker: Element-wise Active Information Acquisition with Bayesian Deep Latent Gaussian Model

Wenbo Gong^{1*}

WG242@CAM.AC.UK

Sebastian Tschiatschek²

SEBASTIAN.TSCHIATSCHEK@MICROSOFT.COM

Richard Turner¹²

RET26@CAM.AC.UK

Sebastian Nowozin^{2†}

NOWOZIN@GMAIL.COM

José Miguel Hernández-Lobato¹²

JMH233@CAM.AC.UK

Cheng Zhang²

CHENG.ZHANG@MICROSOFT.COM

¹*Department of Engineering, University of Cambridge, Cambridge, UK*

²*Microsoft Research, Cambridge, UK*

Abstract

In this paper we introduce the *ice-start* problem, i.e., the challenge of deploying machine learning models when only little or no training data is initially available, and acquiring each feature element of data is associated with costs. This setting is representative for the real-world machine learning applications. For instance, in the health-care domain, when training an AI system for predicting patient metrics from lab tests, obtaining every single measurement comes with a high cost. Active learning, where only the label is associated with a cost does not apply to such problem, because performing all possible lab tests to acquire a new training datum would be costly, as well as unnecessary due to redundancy. We propose *Icebreaker*, a principled framework to approach the ice-start problem. *Icebreaker* uses a full *Bayesian Deep Latent Gaussian Model (BELGAM)* with a novel inference method. Our proposed method combines recent advances in amortized inference and stochastic gradient MCMC to enable fast and accurate posterior inference. By utilizing BELGAM’s ability to fully quantify model uncertainty, we also propose two information acquisition functions for *imputation* and *active prediction* problems. We demonstrate that BELGAM performs significantly better than the previous VAE (Variational autoencoder) based models, when the data set size is small, using both machine learning benchmarks and real-world recommender systems and health-care applications. Moreover, based on BELGAM, *Icebreaker* further improves the performance and demonstrate the ability to use minimum amount of the training data to obtain the highest test time performance.

1. Introduction

Acquiring information is costly in many real-world applications. For example, to make a correct diagnosis and perform effective treatment, a medical doctor often needs to carry out a sequence of medical tests to gather information. Performing each of these tests is associated with a cost in terms of money, time, and health risks. To this end, an AI system

* Contributed during his internship in Microsoft Research

† Now at Google AI, Berlin, Germany (contributed while being with Microsoft Research)

Correspondence to: Cheng Zhang and Wenbo Gong

should be able to suggest the information to be acquired in the form of "one measurement (feature) at a time" to enable the accurate predictions (diagnosis) for any new users/patients. Recently, test-time active prediction methods, such as EDDI (Efficient Dynamic Discovery of high-value Inference) (Ma et al., 2019), provide a solution for when there is sufficient amount of training data available. Unfortunately, in these scenarios, training data can be also challenging and costly to obtain. For example, new data needs to be collected by taking measurements of currently hospitalized patients with their consent. Ideally, we would like to deploy an AI system, such as EDDI when no or only limited training data is available. We call this problem the *ice-start* problem. It is desired to have a method to actively selected training data-element for such task.

The key to address the ice-start problem is to have a scalable model which knows what it does not know, aka to quantify the epistemic uncertainty. In this way, this uncertainty can be used to guide the acquisition of training data, e.g., it would prefer to acquire unfamiliar but informative feature elements over others, such as the familiar but uninformative ones. Thus, such an approach can reduce the cost of acquiring training data. We refer to this as element-wise training-time active acquisition.

Training-time active acquisition is needed in a great range of applications. Apart from general prediction tasks, such as the above health care example, general imputation tasks such as recommender system also need to address the ice-start problem. For example, when a new shop need a recommender where no historical customer data is available. Thus, a framework that can handle different type of tasks is desired.

Despite the success of element-wise test-time active prediction (Ma et al., 2019; Lewenberg et al., 2017; Shim et al., 2018; Zannone et al., 2019), few works have provided a general and scalable solutions for the problem of *ice-start*. Additionally, these works (Melville et al., 2004; Krause and Horvitz, 2010; Krumm and Horvitz, 2019) commonly are limited in a specific application scenario. An element-wise method needs to handle partial observations at any time. More importantly, we need to design new acquisition functions that takes the model parameter uncertainty into account.

In this work, we propose *Icebreaker*, a principled framework to solve the ice-start problem. *Icebreaker* actively acquires informative feature elements during training and also perform active test prediction with small amount of data for training. To enable Icebreaker, we contribute:

- We propose a Bayesian deep Latent Gaussian Model (BELGAM). Standard training of the deep generative model cares about the point estimates for the parameters, whereas our approach applies a fully Bayesian treatment to the weights. Thus, during the training time acquisition, we can leverage the epistemic uncertainty. (Section 2)
- We design a novel partial amortized inference method for BELGAM, naming PA-BELGAM. We combine recent advances in amortized inference for the local latent variables and stochastic gradient MCMC for the model parameters, i.e. the weights of the neural network, to ensure high inference accuracy. (Section 2.2)
- To complete Icebreaker, we propose two training-time information acquisition functions based on the uncertainties modeled by PA-BELGAM to identify informative elements. One acquisition function is designed for imputation tasks (Section 3), and the other for active prediction tasks. (Section 4)

- We evaluate the proposed PA-BELGAM as well as the entire Icebreaker approach on well-used machine learning benchmarks and a real-world health-care task. The method demonstrates clear improvements compared to multiple baselines and shows that it can be effectively used to solve the ice-start problem. (Section 5)

2. Bayesian Deep Latent Gaussian Model (BELGAM) with Partial Amortized Inference

As discussed before, to enable a generic and scalable solution for the Ice-start problem. We first need a flexible model with epidemic uncertainty quantification which can also handle missing values in the data. Here, we propose Bayesian Deep Latent Gaussian Model (BELGAM) with scaleable and accurate approximate inference.

2.1 Bayesian Deep Latent Gaussian Model (BELGAM)

We design a flexible full Bayesian model which provides the model uncertainty quantification. A Bayesian latent variable generative model as shown in Figure 1 is a common choice, but previous work of such models are typically linear and not flexible enough to model highly complex data. A Deep Latent Gaussian Model which uses a neural network mapping is flexible but not fully Bayesian as the uncertainty of the model itself is ignored. We thus propose a Bayesian Deep Latent Gaussian Model (BELGAM), which uses a Bayesian neural network to generate observations \mathbf{X}_O from local latent variables Z with global latent weights θ shown in 1. The model is thus defined as:

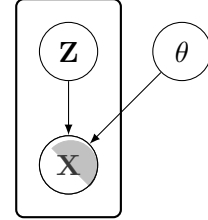


Figure 1: BELGAM

$$p(\mathbf{X}_O, \theta, \mathbf{Z}) = p(\theta) \prod_{i=1}^{|\mathcal{O}|} \prod_{d \in \mathcal{O}_i} p(x_{i,d} | z_i, \theta) p(z_i), \quad (1)$$

where $|\mathcal{X}_O|$ is the observed data. The goal is to infer the posterior, $p(\theta, \mathbf{Z} | \mathbf{X}_O)$, for both local latent variable $\mathbf{Z} = [z_1, \dots, z_{|\mathcal{O}|}]$ and global latent weights θ . Given the posterior, we can infer the missing data as in (Ma et al., 2019). Such a model is generally intractable and approximate inference is needed (Zhang et al., 2018; Li, 2018). Variational inference (VI) (Wainwright et al., 2008; Zhang et al., 2018; Jordan et al., 1999; Beal et al., 2003; Li, 2018) and sampling-based methods (Andrieu et al., 2003) are two types of approaches used for this task. Sampling-based approaches are known for accurate inference performances and theoretical guarantees.

However, sampling the local latent variable \mathbf{Z} is computationally expensive as the cost scales linearly with the data set size. To best trade off the computational cost against the inference accuracy, we propose to amortize the inference for \mathbf{Z} and keep an accurate sampling-based approach for the global latent weights θ . Specifically, we use preconditioned stochastic gradient Hamiltonian Monte Carlo (SGHMC) (Chen et al., 2016) (see appendix for details).

2.2 Partial Amortized BELGAM

Revisiting amortized inference in the presence of missing data. Amortized inference (Kingma and Welling, 2014; Rezende et al., 2014) is an efficient extension for variational inference. It was originally proposed for deep latent Gaussian models where only local latent variables \mathbf{Z} need to be inferred. Instead of using an individually parametrized approximation $q(\mathbf{z}_i)$ for each data instance \mathbf{x}_i , amortized inference uses a deep neural network as a function estimator to compute $q(\mathbf{z}_i)$ using \mathbf{x}_i as input, $q(\mathbf{z}_i|\mathbf{x}_i)$. Thus, the estimation of the local latent variable does not scale with data set size during model training.

However, in our problem setting, the feature values for each data instance are partially observed. Thus, the vanilla amortized inference cannot be used as the input dimensionality to the network can vary for each data instance. As with the Partial VAE proposed in Ma et al. (2019), we adopt the set encoding structure (Qi et al., 2017; Zaheer et al., 2017) to build the inference network to infer \mathbf{Z} based on partial observations in an amortized manner.

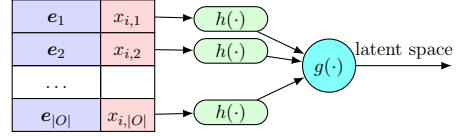


Figure 2: The illustration of P-VAE inference network structure.

As shown in Figure 2, for each data instance $\mathbf{x}_i \in \mathbf{X}_O$ with $|o_i|$ observed features, the input is modified as $\mathbf{S}_i = [\mathbf{s}_{i,1}, \dots, \mathbf{s}_{i,|o_i|}]$ where $\mathbf{s}_{i,d} = [x_{i,d}, \mathbf{e}_d]$ and \mathbf{e}_d is the feature embedding. This is fed into a standard neural network $h(\cdot) : \mathbb{R}^{M+1} \rightarrow \mathbb{R}^K$ where M and K are the dimensions of the latent space and \mathbf{e}_d respectively. Finally, a permutation invariant set function $g(\cdot)$ is applied. In this way, we build an inference network structure that is compatible with partial observations.

Amortized inference + SGHMC As discussed previously, we want to be computationally efficient when inferring \mathbf{Z} and be accurate when inferring the global latent weights θ for BELGAM. Thus, we start with VI and then nest SGHMC into it. Assume we have the factorized approximated posterior $q(\theta, \mathbf{Z}|\mathbf{X}_O) \approx q(\theta|\mathbf{X}_O)q_\phi(\mathbf{Z}|\mathbf{X}_O)$ (Kingma and Welling, 2014; Ma et al., 2019), then the proposed inference scheme can be summarized into two stages: (i) Sample $\theta \sim q(\theta|\mathbf{X}_O)$ using SGHMC, (ii) Update the amortized inference network $q_\phi(\mathbf{z}_i|\mathbf{x}_i)$ to approximate $p(\mathbf{z}_i|\mathbf{x}_i)$.

First, we present how to sample $\theta \sim q(\theta|\mathbf{X}_O)$ using SGHMC. The optimal form for $q(\theta|\mathbf{X}_O)$ can be defined as $q(\theta|\mathbf{X}_O) = \frac{1}{C} e^{\log p(\mathbf{X}_O, \theta)}$, where C is the normalization constant $p(\mathbf{X}_O)$. In order to sample from such optimal distribution, the key is to compute the gradient $\nabla_\theta \log p(\mathbf{X}_O, \theta)$. Unfortunately, this is intractable due to marginalizing the latent variable \mathbf{Z} . Instead, we propose to approximate this quantity by transforming the marginalization into an optimization:

$$\log p(\mathbf{X}_O, \theta) \geq \sum_{i \in \mathbf{X}_O} \left[\mathbb{E}_{q_\phi(\mathbf{z}_i|\mathbf{x}_i)} [\log p(\mathbf{x}_i|\mathbf{z}_i, \theta)] - KL[q_\phi(\mathbf{z}_i|\mathbf{x}_i)||p(\mathbf{z}_i)] \right] + \log p(\theta). \quad (2)$$

We call the right hand side of Eq. 2 as $\mathcal{L}_{joint}(\mathbf{X}_O; \phi)$. Therefore, the marginalization of \mathbf{Z} is transformed into an optimization problem

$$\nabla_\theta \log p(\mathbf{X}_O, \theta) = \nabla_\theta \max_{q_\phi \in \mathcal{F}} \sum_{i \in \mathbf{X}_O} \left[\mathbb{E}_{q_\phi(\mathbf{z}_i|\mathbf{x}_i)} [\log p(\mathbf{x}_i|\mathbf{z}_i, \theta)] - KL[q_\phi(\mathbf{z}_i|\mathbf{x}_i)||p(\mathbf{z}_i)] \right] + \log p(\theta). \quad (3)$$

where \mathcal{F} is a sufficiently large function class.

After sampling θ , we update the inference network with these samples by optimizing:

$$\begin{aligned} \mathcal{L}(\mathbf{X}_O; \phi) &= \mathbb{E}_{q(\theta, \mathbf{Z} | \mathbf{X}_O)}[\log p(\mathbf{X}_O | \mathbf{Z}, \theta)] - KL[q(\mathbf{Z}, \theta | \mathbf{X}_O) || p(\mathbf{Z}, \theta)] \\ &= \mathbb{E}_{q(\theta | \mathbf{X}_O)} \left[\sum_{i \in \mathbf{X}_O} \mathbb{E}_{q_\phi(\mathbf{z}_i | \mathbf{x}_i)}[\log p(\mathbf{x}_i | \mathbf{z}_i, \theta)] - KL[q_\phi(\mathbf{z}_i | \mathbf{x}_i) || p(\mathbf{z}_i)] \right] - KL[q(\theta | \mathbf{X}_O) || p(\theta)]. \end{aligned} \tag{4}$$

where the outer expectation can be approximated by SGHMC samples. The resulting inference algorithm resembles an iterative update procedure, like *Monte Carlo Expectation Maximization* (MCEM) (Wei and Tanner, 1990) where it samples latent \mathbf{Z} and optimizes θ instead. We call the proposed model *Partial Amortized BELGAM* (PA-BELGAM). Partial VAE is actually a special case of PA-BELGAM, where θ is a point estimate instead of a set of samples.

Note that, in this way, the computational cost with single chain SGHMC is exactly the same as training a normal VAE thanks to the amortization for \mathbf{Z} . Thus, PA-BELGAM scales to large data when needed. The only additional cost is the memory for storing θ samples. Thus, we adopt a similar idea based on the Moving Window MCEM algorithm (Havasi et al., 2018), where samples are stored and updated in a fixed size pool with a first in first out (FIFO) procedure. In the next two sections, we present Icebreaker which utilize BELGAM for two general machine learning tasks separately: imputation tasks and prediction tasks.

3. Icebreaker for Imputation Tasks

We present Icebreaker for the imputation task first as the PA-BELGAM can be directly applied, such as recommender in the same way as Ma et al. (2018). We introduce the problem formulation first which provide an overview of the the method. We then present our proposed the active training acquisition function in detail.

3.1 Problem Definition

Assume at each training acquisition step we have training data \mathcal{D}_{train} , a pool data set \mathcal{D}_{pool} that contain the data we could query and $\mathcal{D}_{train} \cup \mathcal{D}_{pool} = \mathbf{X} \in \mathbb{R}^{N \times D}$. In the ice-start scenario, $\mathcal{D}_{train} = \emptyset$. At each step of the training-time acquisition, we actively select data

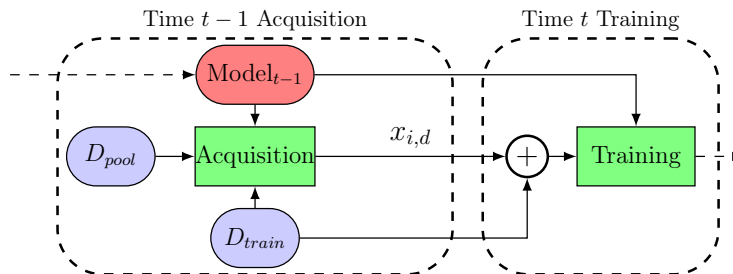


Figure 3: The flow diagram of active training phase at time $t - 1$.

points $x_{i,d} \in \mathcal{D}_{pool}$ to acquire, thereby moving them into \mathcal{D}_{train} and updating the model with the newly formed \mathcal{D}_{train} . Figure 3 shows the flow diagram of this procedure. During the process, at any step, there is an observed data set \mathbf{X}_O (e.g. for training data set $\mathbf{X}_O = \mathcal{D}_{train}$) and unobserved set \mathbf{X}_U with $|O|$ and $|U|$ number of rows respectively. For each (partially observed) data instance $\mathbf{x}_i \in \mathbf{X}_O$, we have the observed index set O_i containing index of observed features for row i . The training time acquisition procedure is summarised in algorithm 1 and Figure 3.

Algorithm 1: Element-wise training time acquisition

```

input :  $\mathbf{X}_O, \mathbf{X}_U, \Phi, \mathcal{M}$ , Acquisition number  $K$ 
/* Initialization */
 $\mathbf{X}_O = \emptyset$ ;
while  $\mathbf{X}_U \neq \emptyset$  do
    /* Information acquisition */
    Compute reward  $R(x_{i,d}, \mathbf{X}_O)$  for  $x_{i,d} \in \mathbf{X}_U$  using Eq.5 or 10 ;           // Reward
    computation
    Sample  $\mathbf{X}_{new}$  ; // Sample  $K$  feature elements according to the  $R$  value.
     $\mathbf{X}_O = \mathbf{X}_O \cup \mathbf{X}_{new}$ ; // Update training set
    /* Model Training */
    Re-initialized the model  $\mathcal{M}$  ; // Re-initialization to avoid local optimum
     $\mathcal{M} = \text{Train}(\mathcal{M}, \Xi)$ ;
    /* Test task */
    Test( $\mathcal{M}$ ); // Test performance of the current model  $\mathcal{M}$ 
end

```

Algorithm 2: Imputation task evaluation

```

Result : Evaluation metric  $p$ 
input :  $\mathcal{D}_O, \mathcal{D}_U, \mathcal{M}, f(\cdot)$ 
 $\hat{\mathcal{D}}_U = \text{Impute}(\mathcal{M}, \mathcal{D}_O)$ ; // Imputation
Compute  $p = f(\mathcal{D}_U)$ 

```

For training acquisition notations, we denote the training set $\mathcal{D}_{train} = \mathbf{X}_O$ and the pool set $\mathcal{D}_{pool} = \mathbf{X}_U$. The model \mathcal{M} training hyper-parameters are grouped as Ξ . We also have the selection method $\text{Update}(\mathbf{X}_O, \mathbf{X}_U, K)$ which picks K values from the pool into the training set using the acquisition described in below. The evaluation methods for the test task is denoted as $\text{Test}(\mathcal{M})$, which is algorithm 2. \mathcal{D}_O and \mathcal{D}_U represents the observed/unobserved test data. $f(\cdot)$ is the evaluation metric e.g. negative log likelihood (NLL).

3.2 Active Information Acquisition for Imputation

Designing the training time acquisition function is not trivial at all. Some of the previous work focus on developing intuition-based acquisition functions such as variance of the feature value (Huang et al., 2018) or expected improvement of the model (Melville et al., 2005). On the other hand, the recent proposed acquisition, EDDI (Ma et al., 2019) is a valid information-theoretic objective. However, it is under the assumptions that the model is well trained and only test-time feature acquisition is performed, thus, this is not directly

applicable in our formulation (see appendix C.1 for details). The ideal acquisition should balance the reduction of the model uncertainty and performance of the desired task.

Imputing missing values is important to applications such as recommender systems and other down-stream tasks. In this setting, the goal is to learn about all the features elements (item user pairs in the recommender system setting) as quickly as possible. This can be formalized as selecting the elements $x_{i,d}$ that maximize the expected reduction in the posterior uncertainty of θ :

$$R_I(x_{i,d}, \mathbf{X}_O) = H[p(\theta|\mathbf{X}_O)] - \mathbb{E}_{p(x_{i,d}|\mathbf{X}_O)}[H[p(\theta|\mathbf{X}_O, x_{i,d})]]. \quad (5)$$

We use the symmetry of mutual information to sidestep the posterior update $p(\theta|\mathbf{X}_O, x_{i,d})$ and entropy estimation of θ for efficiency. Thus, Eq. 5 is written as

$$R_I(x_{i,d}, \mathbf{X}_O) = H[p(x_{i,d}|\mathbf{X}_O)] - \mathbb{E}_{p(\theta|\mathbf{X}_O)}[H[p(x_{i,d}|\theta, \mathbf{X}_O)]]. \quad (6)$$

We can approximate Eq. 6 as

$$R_I(x_{i,d}, \mathbf{X}_O) \approx -\frac{1}{K} \sum_k \log \frac{1}{MN} \sum_{m,n} p(x_{i,d}^k | z_i^m, \theta^n) + \frac{1}{NK} \sum_{k,n} \log \frac{1}{M} \sum_m p(x_{i,d}^k | z_i^m, \theta^n). \quad (7)$$

based on the samples $\{\theta^n\}_{n=1}^N$, $\{z_i^m\}_{m=1}^M$ and $\{x_{i,d}^k\}_{k=1}^K$ from SGHMC, the amortized inference network and the data distribution respectively. The sample $x_{i,d} \sim p(x_{i,d}|\mathbf{X}_O)$ can be generated in the following way: (i) $z_i \sim q_\phi(z_i|\mathbf{x}_{iO})$ (ii) $\theta \sim q(\theta|\mathbf{X}_O)$ (iii) $x_{i,d} \sim p(x_{i,d}|\theta, z_i)$, where \mathbf{x}_{iO} represents the observed features in i^{th} row of \mathbf{X}_O

4. Icebreaker for Prediction Tasks

Next, we introduce the second type of test task called active prediction, where a target variable is specified and active sequential acquisition is used in the test time. Note that the same framework applies for regular prediction tasks as well. Here, we demonstrate the case where feature wise active information acquisition is used in both training and testing time, which is desired in the data costly situation. Following the same structure of imputation section, we first formally define this problem, and then extend the model used for imputation to active prediction. In the end, a novel acquisition function is proposed.

4.1 Problem Definition

During the training acquisition, the procedure is exactly the same as imputation task, which is shown in algorithm 1 and Figure 3, apart from that we have clear target variables. We denote the target as \mathbf{Y} . In this case, each $\mathbf{x}_i \in \mathbf{X}_O$ has a corresponding target \mathbf{y}_i . In addition, for each training acquisition step, instead of querying single feature value $x_{i,d}$ as the imputation task, we query a feature-target pair $(x_{i,d}, y_i)$ if y_i has not been queried before. Otherwise, we only query $x_{i,d}$.

As the name active prediction suggests, the test task requires the model to actively select features in test pool set to improve the prediction accuracy. Formally, we have an additional test target \mathbf{Y}^* compared to imputation task. At each test time query, a single feature $x_{id}^* \in \mathbf{X}_U^*$ for each row i is moved into \mathbf{X}_O^* . The goal is to achieve better target prediction

$f(\mathbf{Y}^*)$ with minimal data queries in the test time. We use *Area under information curve* (AUIC) as the evaluation metric for this test-time active prediction suggested in EDDI (Ma et al., 2019). The entire active prediction evaluation procedure is summarised in algorithm 3

Algorithm 3: Active prediction task evaluation

Result: Area under information curve AUIC
input : $\mathcal{D}_O, \mathcal{D}_U, \mathcal{M}, f(\cdot), \mathbf{Y}$
 /* Initialization */
 $\mathcal{D}_O = \emptyset;$
 $\text{AUIC} = 0;$
while $\mathcal{D}_U \neq \emptyset$ **do**
 | /* Test time acquisition */
 | Compute EDDI reward $R(x_{i,d}, \mathcal{D}_O)$ for $x_{i,d} \in \mathcal{D}_U$ using Eq.22 for each row i ;
 | Select single $x_{i,d} \in \mathcal{D}_U$ into \mathcal{D}_O for each row i ; // Test time acquisition
 | /* Test Evaluation */
 | Predict $\hat{\mathbf{Y}} = \text{Predict}(\mathcal{M}, \mathcal{D}_O);$ // Prediction
 | Compute $p = f(\mathbf{Y})$; // Evaluation
 | $\text{AUIC} += p;$ // Compute AUIC value
end

4.2 Model and Active Information Acquisition for Active Prediction

Conditional BELGAM In the prediction task, the model needs to incorporate the target variable. The proposed model and inference algorithm in the previous imputation section can be easily extended to incorporate these variables. In general, PA-BELGAM can be adapted in any VAE based framework directly. One possible choice is to adopt the formulation of conditional VAE (Sohn et al., 2015). The details are in appendix B.

Icebreaker for active target prediction. For the prediction task, solely reducing the model uncertainty is not optimal as the goal is to predict the target variable \mathbf{Y} . In this context, we require the model to (1) capture the correlations and accurately impute the unobserved feature values in the pool set because during the test time sequential feature selection, the model needs to estimate the candidate missing element $x_{i,d}$ for decision making, and (2) find informative feature combinations to learn to predict the target variable. Thus, the desired acquisition function needs to trade-off exploring different features to learn their relationships against learning a predictor by exploiting the informative feature combinations. We propose the following objective:

$$R_P(x_{i,d}, \mathbf{X}_O) = \mathbb{E}_{p(x_{i,d}|\mathbf{X}_O)}[H[p(\mathbf{y}_i|x_{i,d}, \mathbf{X}_O)]] - \mathbb{E}_{p(\theta, x_{i,d}|\mathbf{X}_O)}[H[p(\mathbf{y}_i|\theta, x_{i,d}, \mathbf{X}_O)]]. \quad (8)$$

The above objective is equivalent to *conditional mutual information* $I(\mathbf{y}_i, \theta|x_{i,d}; \mathbf{X}_O)$. Thus, maximizing it is the same as maximizing the information to predict the target y_i through the model weights θ , conditioned on the observed features \mathbf{X}_O with this additional feature $x_{i,d}$. In our case, the $x_{i,d}$ is unobserved. As the weights θ do not change significantly over one feature element, for computational convenience we assume $p(\theta|\mathbf{X}_O) \approx p(\theta|\mathbf{X}_O, x_{i,d})$ when estimating the objective.

Similar to Eq. 7, we approximate this objective using Monte Carlo integration:

$$R_P(x_{i,d}, \mathbf{X}_O) \approx -\frac{1}{JK} \sum_{j,k} \log \frac{1}{MN} \sum_{m,n} p(\mathbf{y}_i^{(j,k)} | \mathbf{z}_i^{(m,k)}, \theta^n) + \frac{1}{KNJ} \sum_{j,n,k} \log \frac{1}{M} \sum_m p(\mathbf{y}_i^{(j,k)} | \mathbf{z}_i^{(m,k)}, \theta^n), \quad (9)$$

where we draw $\{\mathbf{z}_i^{(m,k)}\}_{m=1}^M$ from $q_\phi(\mathbf{z}_i | \mathbf{X}_O, x_{i,d}^k)$ for each imputed sample $x_{i,d}^k$. Others ($\{\theta^n\}_{n=1}^N$, $\{\mathbf{y}_i^{(j,k)}\}_{j=1}^J$ and $\{x_{i,d}^k\}_{k=1}^K$) are sampled in a similar way as in the imputation task. This objective naturally balances the exploration among features as well as the exploitation to find informative ones for the prediction task. For example, if feature $x_{i,d}$ is less explored or uninformative about the target, the first entropy term in Eq. 8 will be high, which encourages the algorithm to pick this unfamiliar data. However, using this term alone can result in selecting uninformative/noisy features. Thus, a counter-balance force for exploitation is needed, which is exactly the role of the second term. Unless $x_{i,d}$ together with θ can provide extra information about the target \mathbf{y}_i , the entropy in the second term with uninformative features will still be high. Thus, the two terms combined together encourage the model to select the less explored but informative features. The proposed objective is mainly targeted at the second requirement mentioned at the beginning of this section. However, its effectiveness depends heavily on the imputing quality of $x_{i,d}$. Thus, a natural way to satisfy both conditions is a combination of the two objectives:

$$R_C(x_{i,d}, \mathbf{X}_O) = (1 - \alpha)R_I(x_{i,d}, \mathbf{X}_O) + \alpha R_P(x_{i,d}, \mathbf{X}_O), \quad (10)$$

where α controls which task the model focuses on. This objective also has an information theoretic interpretation. In the appendix C.1, we show that when $\alpha = \frac{1}{2}$, this combined objective is equivalent to the mutual information between θ and the feature-target pair $(x_{i,d}, \mathbf{y}_i)$.

5. Experiments

We evaluate Icebreaker first on machine learning benchmark data sets from UCI (Dheeru and Karra Taniskidou, 2017) on both imputation and prediction tasks. We then evaluate it in two real-world applications: (a) movie rating imputation using *MovieLens* (Harper and Konstan, 2016); (b) risk prediction in intensive care using MIMIC (Johnson et al., 2016).

Experiments Setup and evaluation. We compare the Icebreaker with random feature acquisition strategy for training where both P-VAE (Ma et al., 2019) and PA-BELGAM are used. For the imputation task, P-VAE already achieves excellent results in various data sets compared to traditional methods Ma et al. (2019); Nazabal et al. (2018). Additionally for the active prediction task, we compare the Icebreaker to the instance-wise active learning, denoted as *Row AT*, where the data are assumed to be fully observed apart from the target.

We evaluate the imputation performance by reporting *negative log likelihood* (NLL) over the test target. For the active prediction task, we use EDDI (Ma et al., 2019) to sequentially select features at test time. We report the *area under information curve* (AUIC) (Ma et al., 2019) for the test set (See Figure 5 for example and appendix for details). A smaller value of AUIC indicates better overall active prediction performance. All experiments are averaged over 10 runs and their setting details are in the appendix.

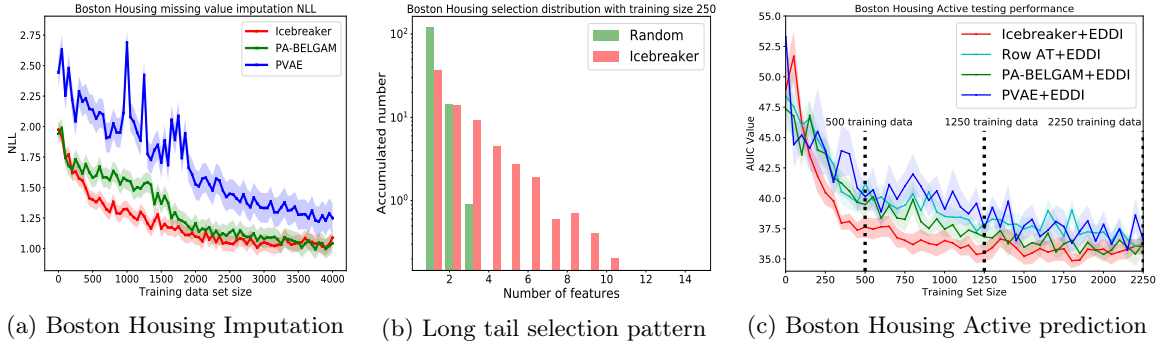


Figure 4: Boston Housing experimental results. (a) The NLL over the number of observed feature values. (b) The distribution of the number of the feature for data instance during the training time. (c) Performance of the active prediction task over number of training data elements. The test time active prediction curves with the training data size indicated by black dash line are shown in Figure 5

5.1 UCI Data Set

Imputation Task. At each step of Icebreaker we select 50 feature elements from the pool. Figure 4a shows the NLL on the test set as the training set increases. Icebreaker outperforms random acquisition with both PA-BELGAM and P-VAE by a large margin, especially at early stages of training. We also see that PA-BELGAM alone can be beneficial compared to P-VAE with small data set. This is because P-VAE tends to over-fit, while PA-BELGAM leverages the model uncertainties.

We also analyze the feature selection pattern of the Icebreaker. We gather all the rows that have been queried with at least one feature during training acquisition and count how many features are queried for each. We repeat this for the first 5 acquisitions. Figure 4b shows the histogram of the number of features acquired for each data point. The random selection concentrates around 1 feature per data instance. However, the long-tailed distribution of the number of selected features of Icebreaker means it tends to exploit the correlations between features inside certain rows but simultaneously tries to spread its selection for more exploration. We include the imputation results on other UCI data set in the Appendix. We find that Icebreaker consistently outperforms the baseline by a large margin.

Prediction Task. Figure 4c shows the AUIC curve as the amount of training data increases. The Icebreaker clearly achieves better results compared to all baselines (Also confirmed by Figure 5). This shows that it not only has a more accurate prediction of the targets but also captures correlations between features and targets. Interestingly, the baseline *Row AT* performs a little worse than PA-BELGAM. We argue this is because it is wasteful to query the whole row, especially with a fixed query budget. Thus, it will form a relatively small but complete data set. Again, the uncertainty of PA-BELGAM brings benefits compared to P-VAE with point estimated parameters.

We confirm our guess by plotting the active test NLL curve as (Ma et al., 2019) in Figure 5. At the early training stage (500 data points, left panel in Figure 5), the performance of *Row AT* is worse in the test time than others when few features are selected. This is due to

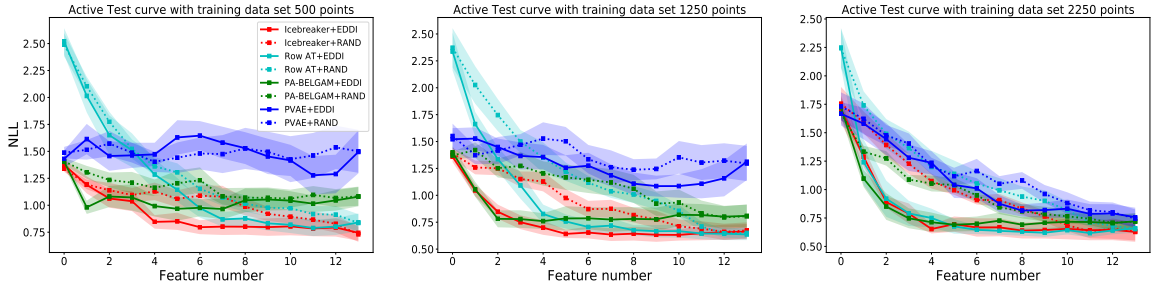


Figure 5: Evaluation of test time performance after exposure to different number of training data: **(Left)**: 550 feature elements. **(Middle)**:1250 feature elements **(Right)**: 2250 feature elements. The x-axis indicates the number of features elements used for prediction. Legend indicates the methods used for training (Icebreaker, Row AT, etc.) and test time acquisition (EDDI, RAND)

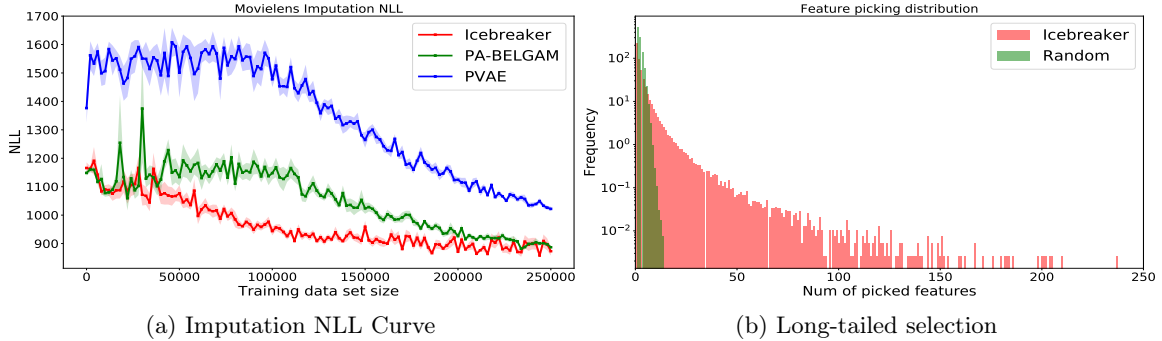


Figure 6: Performance using MovieLens. Panel (a) shows the imputation NLL with number of observed movie ratings. Panel (b) shows the distribution of the number of features selected for each user).

obtaining a complete observed datum is costly. With the budget of 500 feature element, it can only select 50 fully observed data instances. In contrast, Icebreaker has obtained 260 partially observed instances with different level of missingness. As more features are selected during test, these issues are mitigated and the performance starts to improve. Further evidence suggests that, as the training data grows, we can clearly observe a better prediction performance of *Row AT* at the early test stage. We also include the evaluation of our method on other UCI data for active prediction in the appendix.

5.2 Recommender System using MovieLens

One common benchmark data set for recommender systems is *MovieLens-1M* (Harper and Konstan, 2016). P-VAE has obtained the state-of-the-art imputation performance after training with sufficient amount of data (Ma et al., 2018). Figure 6a shows the performance on predicting unseen items in terms of NLL. Icebreaker shows that with minimum data, the model has learned to predict the unseen data. Given any small amount of data, Icebreaker

obtains the best performance at the given query budget, followed by PA-BELGAM which outperforms P-VAE. The selection pattern is similar to the UCI imputation, shown in Figure 6b. We argue this long tail selection is important especially when each row contains many features. The random selection tends to scatter the choices and is less likely to discover dependencies until the data set grows larger. But if there are many features per data instance, this accumulation will take very long time. On the other hand, the long-tailed selection exploits the features inside certain rows to discover their dependencies and simultaneously tries to spread out the queries for exploration.

5.3 Mortality Predicting using MIMIC

We apply the Icebreaker to a health-care application using the Medical Information Mart for Intensive Care (MIMIC III) data set (Johnson et al., 2016). This is the largest real-world healthcare data set in terms of the patient number. The goal is to predict the mortality based on the 17 medical measurements. The data is pre-processed following Harutyunyan et al. (2017) and balanced. Full details are available in the appendix D.2.1.

The left panel in Figure 7 shows that the Icebreaker outperforms the other baselines significantly with higher robustness (smaller std. error). Robustness is crucial in health-care settings as the cost of unstable model performance is high. Similarly, *Row AT* performs more poorly until it accumulates sufficient data. Note that without active training feature selection, PA-BELGAM performs better than P-VAE due to its ability to model uncertainty given this extremely noisy data set.

To evaluate whether the proposed method can discover valuable information, we plot the accumulated feature number in the middle panel of Figure 7. The x-axis indicates the total number of points in the training set and each point on the curve indicates the feature selection number in the training set. We see that not only different features have been collected at different frequency, the curve of the accumulated feature such as Glucose is clearly non-linear as well. This indicates that the importance of different feature varies at different training phases. Icebreaker is establishing a sophisticated feature element acquisition scheme that no heuristic method can currently achieve. The top 3 features are the *Glasgow coma scale* (GCS). These features have been identified previously as being clinically important (e.g. by the IMPACT model (Steyerberg et al., 2008)). *Glucose* is also in the IMPACT set. It was not collected frequently in the early stage, but in the later training phase, more *Glucose* has been selected. Compared to GCS, Glucose has a highly non-linear relationship with the patient outcome (Popkes et al., 2019) (or refer to the appendix D.2.1). Icebreaker chooses more informative features with simpler relationship in the very early iteration. While the learning progresses, Icebreaker is able to identify these informative features with complex relationship to the target. Additionally, the missing rate for each feature in the entire data set differs. *Capillary refill rate* (*Cap.*) has more than 90% data missing, much higher than *Height*. Icebreaker is still able to pick the useful and rarely observed information, while only chooses a small percent of the irrelevant information during the test. On the right hand side of Figure 7, we plot the histogram of the initial choices during test-time acquisition. *GCS* are mostly selected in the first step as it is the most informative feature.

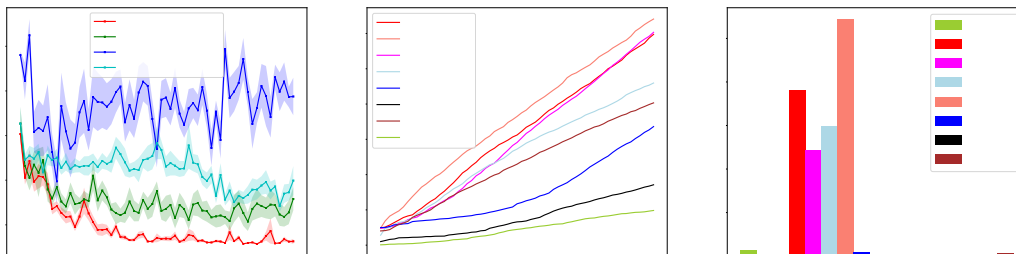


Figure 7: Performance of MIMIC experiments. **(Left)** This figure shows the predictive AUIC curve as training data size increases. **(Middle)** The accumulated feature statistics as active selection progresses **(Right)** This indicates the histogram of initial choice during active prediction using EDDI.

6. Related Work

Data-wise Active Learning. The goal of active learning is to obtain optimal model performance with as fewer queries as possible (MacKay, 1992; Settles, 2012; McCallumzy and Nigamy, 1998), where only querying labels are associated with a cost. One category is based on decision theory (Roy and McCallum), where acquisition step is to minimize the loss defined by test tasks after making the query based on observed data. Indeed this is the optimal objective as it coincides perfectly with the goal of active learning. However, the evaluation of this objective can be expensive in practice (Kapoor et al.; Zhu et al.). Furthermore, it is task and model dependent, which makes it difficult to be applied in situations where test loss or distribution is unknown in advance. Another category is based on information theory which is model and data set agnostic. Many previous active learning approaches are in this category. For example, Tong and Koller (2001) proposed margin sampling based on heuristics, and Cover and Thomas (2012); Lindley (1956) quantifies the uncertainty using KL divergence. Another well-known acquisition function is BALD (Houlsby et al., 2011) which is based on mutual information. Although our proposed acquisition for imputation is also based on mutual information, we emphasize that the original BALD objective is only applied to scenarios where the data set has fully observed inputs and target variables. In other words, those methods aim to only select next data point to label while assuming that every feature of each data point is observed. We call this approach *instance-wise* selection. Obviously, these methods are not directly applicable to the settings considered here as they assume that the only cost comes from acquiring labels. This is not the case in many real-world applications as any information acquisition is typically costly.

Feature-wise Active Learning. Instead of only querying labels, the above active learning idea can be extended to query features, named as active feature acquisition (AFA). It makes sequential feature selections in order to improve model performance (Melville et al., 2004; Saar-Tsechansky et al., 2009; Thahir et al., 2012). One category of these methods is based on estimating the expected improvement of the model, e.g. classification (Melville et al., 2005) and clustering (Vu et al.). However, this type of method is task specific and also expensive to compute. Another category of AFA is based on matrix completion. For example, in some cases, the observed features in a matrix are not enough to recover the missing entries. Thus,

there are some active learning approaches proposed to query the most informative one for completion (Chakraborty et al., 2013). In (Sutherland et al., 2013), it queries the features for collaborative prediction using variational approximation of the posterior distribution, and (Ruchansky et al., 2015) unifies the active querying and matrix completion. Instead of using low rank assumption for matrix completion, (Huang et al., 2018) utilizes the supervised information from a classification model to complete the matrix and propose a variance based feature acquisition function. However, the above methods cannot be used for *ice-start* problem as they either cannot handle prediction tasks (e.g. active matrix completion) or requires fully observed test input (Huang et al., 2018), i.e. they cannot solve *active-prediction* problem. In addition, the feature acquisition function is also based on heuristics, which does not take *aleoteric* uncertainty into account. Instead of actively selecting feature for training, Ma et al. (2019) designs an information acquisition function to allow scalable active selection during test time. Shim et al. (2018); Janisch et al. (2017) use a RL-based decision making to actively select test features. However, these methods can only do active learning at test time and requires a large amount of training data. Our framework aims to principally combine the these two tasks. Namely, it can perform test-time active predictions but also can actively select training points from the very beginning, even in an ice-start situation.

Cold-start problem Another relevant problem to *ice-start* is called *cold-start* problem (Maltz and Ehrlich; Schein et al., 2002). The key difference between these two scenarios is that cold-start problem targets at the test time data scarcity after the model has been trained. Take recommender system as an example, the cold-start problem handles the scenario when there are new users incoming with no historical ratings, and the aim is to improve the recommendation quality for these new users. One common strategy is to utilise the meta data (e.g. user profiles, item category) to initialise the latent factors of users/items. Xu et al. (2015); Pandey and Rajpoot (2016) initialized the users’ latent factor by comparing the meta data of the new user with the old ones. On the other hand, Houlsby et al. (2014) uses matrix factorization and information acquisition function to query the preference of the new user without using any meta data. However, one common assumption of these above methods is that the model is well-trained under sufficient amount of training data, which is not available under *ice-start* scenario.

7. Conclusion

In this work, we introduce the ice-start problem where machine learning models are expected to be deployed where little or no training data has been collected. The costs of collecting new training datum apply at the level of feature elements. Icebreaker provides an information theoretical way to actively acquire element-wise data for training and uses the minimum amount of data for downstream test tasks like *imputation* and *active prediction*. Within the framework of *Icebreaker*, we propose PA-BELGAM, a Bayesian deep latent Gaussian model together with a novel inference scheme that combines amortized inference and SGHMC. This enables fast and accurate posterior inference. Furthermore, we propose two training time acquisition functions targeted at the *imputation* and *active prediction* tasks. We evaluate *Icebreaker* on several benchmark data sets including two real-world applications. Icebreaker consistently outperforms the baselines. Possible future directions include taking the mixed-type variables into account and deploying it in a pure streaming environment.

References

- Christophe Andrieu, Nando De Freitas, Arnaud Doucet, and Michael I Jordan. An introduction to MCMC for machine learning. *Machine learning*, 50(1-2):5–43, 2003.
- Yoram Baram, Ran El Yaniv, and Kobi Luz. Online choice of active learning algorithms. *Journal of Machine Learning Research*, 5(Mar):255–291, 2004.
- Matthew James Beal et al. *Variational algorithms for approximate Bayesian inference*. 2003.
- José M Bernardo. Expected information as expected utility. *The Annals of Statistics*, pages 686–690, 1979.
- Shayok Chakraborty, Jiayu Zhou, Vineeth Balasubramanian, Sethuraman Panchanathan, Ian Davidson, and Jieping Ye. Active matrix completion. In *2013 IEEE 13th International Conference on Data Mining*, pages 81–90. IEEE, 2013.
- Changyou Chen, David Carlson, Zhe Gan, Chunyuan Li, and Lawrence Carin. Bridging the gap between stochastic gradient MCMC and stochastic optimization. In *Artificial Intelligence and Statistics*, pages 1051–1060, 2016.
- Thomas M Cover and Joy A Thomas. *Elements of information theory*. John Wiley & Sons, 2012.
- Dua Dheeru and Efi Karra Taniskidou. UCI machine learning repository, 2017. URL <http://archive.ics.uci.edu/ml>.
- Yarin Gal, Riashat Islam, and Zoubin Ghahramani. Deep bayesian active learning with image data. In *Proceedings of the 34th International Conference on Machine Learning-Volume 70*, pages 1183–1192. JMLR. org, 2017.
- F Maxwell Harper and Joseph A Konstan. The Movielens datasets: History and context. *Acm transactions on interactive intelligent systems (tiis)*, 5(4):19, 2016.
- Hrayr Harutyunyan, Hrant Khachatrian, David C Kale, and Aram Galstyan. Multitask learning and benchmarking with clinical time series data. *arXiv preprint arXiv:1703.07771*, 2017.
- Marton Havasi, José Miguel Hernández-Lobato, and Juan José Murillo-Fuentes. Inference in deep gaussian processes using stochastic gradient Hamiltonian Monte Carlo. In *Advances in Neural Information Processing Systems*, pages 7506–7516, 2018.
- Neil Houlsby, Ferenc Huszár, Zoubin Ghahramani, and Máté Lengyel. Bayesian active learning for classification and preference learning. *arXiv preprint arXiv:1112.5745*, 2011.
- Neil Houlsby, José Miguel Hernández-Lobato, and Zoubin Ghahramani. Cold-start active learning with robust ordinal matrix factorization. In *International Conference on Machine Learning*, pages 766–774, 2014.

- Sheng-Jun Huang, Miao Xu, Ming-Kun Xie, Masashi Sugiyama, Gang Niu, and Songcan Chen. Active feature acquisition with supervised matrix completion. *arXiv preprint arXiv:1802.05380*, 2018.
- Jaromír Janisch, Tomáš Pevný, and Viliam Lisý. Classification with costly features using deep reinforcement learning. *arXiv preprint arXiv:1711.07364*, 2017.
- Alistair EW Johnson, Tom J Pollard, Lu Shen, H Lehman Li-wei, Mengling Feng, Mohammad Ghassemi, Benjamin Moody, Peter Szolovits, Leo Anthony Celi, and Roger G Mark. MIMIC-III, a freely accessible critical care database. *Scientific Data*, 3:160035, 2016.
- Michael I Jordan, Zoubin Ghahramani, Tommi S Jaakkola, and Lawrence K Saul. An introduction to variational methods for graphical models. *Machine learning*, 37(2):183–233, 1999.
- Ashish Kapoor, Eric Horvitz, and Sumit Basu. Selective supervision: Guiding supervised learning with decision-theoretic active learning.
- Diederik P Kingma and Max Welling. Auto-encoding variational Bayes. In *International Conference on Learning Representation*, 2014.
- Andreas Krause and Eric Horvitz. A utility-theoretic approach to privacy in online services. *Journal of Artificial Intelligence Research*, 39:633–662, 2010.
- John Krumm and Eric Horvitz. Traffic updates: Saying a lot while revealing a little. 2019.
- Yoad Lewenberg, Yoram Bachrach, Ulrich Paquet, and Jeffrey S Rosenschein. Knowing what to ask: A Bayesian active learning approach to the surveying problem. In *AAAI*, pages 1396–1402, 2017.
- Chunyuan Li, Changyou Chen, David Carlson, and Lawrence Carin. Preconditioned stochastic gradient Langevin dynamics for deep neural networks. In *Thirtieth AAAI Conference on Artificial Intelligence*, 2016.
- Yingzhen Li. *Approximate Inference: New Visions*. PhD thesis, University of Cambridge, 2018.
- Dennis V Lindley. On a measure of the information provided by an experiment. *The Annals of Mathematical Statistics*, pages 986–1005, 1956.
- Chao Ma, Wenbo Gong, José Miguel Hernández-Lobato, Noam Koenigstein, Sebastian Nowozin, and Cheng Zhang. Partial VAE for hybrid recommender system. In *NIPS Workshop on Bayesian Deep Learning*, 2018.
- Chao Ma, Sebastian Tschitschek, Konstantina Palla, Jose Miguel Hernandez Lobato, Sebastian Nowozin, and Cheng Zhang. EDDI: Efficient dynamic discovery of high-value information with partial vae. In *Proceedings of the International Conference on Machine Learning*, 2019.
- David JC MacKay. Information-based objective functions for active data selection. *Neural computation*, 4(4):590–604, 1992.

- David Maltz and Kate Ehrlich. Pointing the way: active collaborative filtering.
- Andrew Kachites McCallumzy and Kamal Nigamy. Employing EM and pool-based active learning for text classification. In *International Conference on Machine Learning*, pages 359–367. Citeseer, 1998.
- Prem Melville, Maytal Saar-Tsechansky, Foster Provost, and Raymond Mooney. Active feature-value acquisition for classifier induction. In *International Conference on Data Mining*, pages 483–486. IEEE, 2004.
- Prem Melville, Maytal Saar-Tsechansky, Foster Provost, and Raymond Mooney. An expected utility approach to active feature-value acquisition. In *Fifth IEEE International Conference on Data Mining (ICDM'05)*, pages 4–pp. IEEE, 2005.
- Alfredo Nazabal, Pablo M Olmos, Zoubin Ghahramani, and Isabel Valera. Handling incomplete heterogeneous data using VAEs. *arXiv preprint arXiv:1807.03653*, 2018.
- Anand Kishor Pandey and Dharmveer Singh Rajpoot. Resolving cold start problem in recommendation system using demographic approach. In *2016 International Conference on Signal Processing and Communication (ICSC)*, pages 213–218. IEEE, 2016.
- Anna-Lena Popkes, Hiske Overweg, Ari Ercole, Yingzhen Li, José Miguel Hernández-Lobato, Yordan Zaykov, and Cheng Zhang. Interpretable outcome prediction with sparse Bayesian neural networks in intensive care. *arXiv preprint arXiv:1905.02599*, 2019.
- Charles R Qi, Hao Su, Kaichun Mo, and Leonidas J Guibas. Pointnet: Deep learning on point sets for 3D classification and segmentation. In *Proceedings of the IEEE Conference on Computer Vision and Pattern Recognition*, pages 652–660, 2017.
- Danilo Jimenez Rezende, Shakir Mohamed, and Daan Wierstra. Stochastic backpropagation and approximate inference in deep generative models. In *International Conference on Machine Learning*, 2014.
- Nicholas Roy and Andrew McCallum. Toward optimal active learning through monte carlo estimation of error reduction.
- Natali Ruchansky, Mark Crovella, and Evimaria Terzi. Matrix completion with queries. In *Proceedings of the 21th ACM SIGKDD International Conference on Knowledge Discovery and Data Mining*, pages 1025–1034. ACM, 2015.
- Maytal Saar-Tsechansky, Prem Melville, and Foster Provost. Active feature-value acquisition. *Management Science*, 55(4):664–684, 2009.
- Andrew I Schein, Alexandrin Popescul, Lyle H Ungar, and David M Pennock. Methods and metrics for cold-start recommendations. In *Proceedings of the 25th annual international ACM SIGIR conference on Research and development in information retrieval*, pages 253–260. ACM, 2002.
- Burr Settles. Active learning. *Synthesis Lectures on Artificial Intelligence and Machine Learning*, 6(1):1–114, 2012.

- Hajin Shim, Sung Ju Hwang, and Eunho Yang. Joint active feature acquisition and classification with variable-size set encoding. In *Advances in Neural Information Processing Systems*, 2018.
- Kihyuk Sohn, Honglak Lee, and Xinchun Yan. Learning structured output representation using deep conditional generative models. In *Advances in neural information processing systems*, pages 3483–3491, 2015.
- Ewout W Steyerberg, Nino Mushkudiani, Pablo Perel, Isabella Butcher, Juan Lu, Gillian S McHugh, Gordon D Murray, Anthony Marmarou, Ian Roberts, J Dik F Habbema, et al. Predicting outcome after traumatic brain injury: development and international validation of prognostic scores based on admission characteristics. *PLoS medicine*, 5(8):e165, 2008.
- Dougal J Sutherland, Barnabás Póczos, and Jeff Schneider. Active learning and search on low-rank matrices. In *Proceedings of the 19th ACM SIGKDD international conference on Knowledge discovery and data mining*, pages 212–220. ACM, 2013.
- Mohamed Thahir, Tarun Sharma, and Madhavi K Ganapathiraju. An efficient heuristic method for active feature acquisition and its application to protein-protein interaction prediction. In *BMC proceedings*, volume 6, page S2. BioMed Central, 2012.
- Simon Tong and Daphne Koller. Support vector machine active learning with applications to text classification. *Journal of machine learning research*, 2(Nov):45–66, 2001.
- Duy Vu, Prem Melville, Mikhail Bilenko, and Maytal Saar-Tsechansky. Intelligent information acquisition for improved clustering.
- Martin J Wainwright, Michael I Jordan, et al. Graphical models, exponential families, and variational inference. *Foundations and Trends® in Machine Learning*, 1(1–2):1–305, 2008.
- Greg CG Wei and Martin A Tanner. A Monte Carlo implementation of the EM algorithm and the poor man’s data augmentation algorithms. *Journal of the American statistical Association*, 85(411):699–704, 1990.
- Jingwei Xu, Yuan Yao, Hanghang Tong, Xianping Tao, and Jian Lu. Ice-breaking: mitigating cold-start recommendation problem by rating comparison. In *Twenty-Fourth International Joint Conference on Artificial Intelligence*, 2015.
- Manzil Zaheer, Satwik Kottur, Siamak Ravanbakhsh, Barnabas Poczos, Ruslan R Salakhutdinov, and Alexander J Smola. Deep sets. In *Advances in Neural Information Processing Systems*, pages 3391–3401, 2017.
- Sara Zannone, José Miguel Hernández-Lobato, Cheng Zhang, and Konstantina Palla. Odin: Optimal discovery of high-value information using model-based deep reinforcement learning. In *ICML Real-world Sequential Decision Making Workshop*, 2019.
- Cheng Zhang, Judith Butepage, Hedvig Kjellstrom, and Stephan Mandt. Advances in variational inference. *IEEE transactions on pattern analysis and machine intelligence*, 2018.

Jia-Jie Zhu and José Bento. Generative adversarial active learning. *arXiv preprint arXiv:1702.07956*, 2017.

Xiaojin Zhu, John Lafferty, and Zoubin Ghahramani. Combining active learning and semi-supervised learning using gaussian fields and harmonic functions.

Appendix A. Stochastic Gradient HMC

Assume we want to draw samples $\theta \sim p(\theta|\mathbf{X}_O)$, the potential energy $U(\theta)$ is defined as (for our partial amortized inference algorithm, this is replaced with Eq. 3)

$$U(\theta) = - \sum_{\mathbf{x}_I \in \mathbf{X}_O} \log p(\mathbf{x}_I|\theta) - \log p(\theta). \quad (11)$$

Typically, we use the mini-batch to estimate this quantity, therefore, the stochastic estimate of $U(\theta)$ with the batch \mathbf{X}_S can be written as

$$\tilde{U}(\theta, \mathbf{X}_S) = - \frac{|O|}{|S|} \sum_{\mathbf{x}_i \in \mathbf{X}_S} \log p(\mathbf{x}_i|\theta) - \log p(\theta), \quad (12)$$

where $|S|$ and $|O|$ are the number of rows for \mathbf{X}_S and \mathbf{X}_O respectively.

The preconditioned SGHMC (Chen et al., 2016) uses the diagonal Fisher information matrix as the adaptive pre-conditioner with moving average approximations (Li et al., 2016). Thus, the transition dynamics at time t is the following :

$$\left. \begin{aligned} B &= \frac{1}{2}\epsilon \\ V_{t-1} &= (1 - \tau)V_{t-2} + \tau \nabla_{\theta} \tilde{U}(\theta) \cdot \nabla_{\theta} \tilde{U}(\theta) \\ g_{t-1} &= \frac{1}{\sqrt{\lambda + \sqrt{V_{t-1}}}} \end{aligned} \right\} \text{Preconditioning Computation} \quad (13)$$

$$\left. \begin{aligned} \mathbf{p}_t &= (1 - \epsilon\beta)\mathbf{p}_{t-1} - \epsilon g_{t-1} \nabla_{\theta} \tilde{U}(\theta) + \epsilon \frac{\partial g_{t-1}}{\partial \theta_{t-1}} + \sqrt{2\epsilon(\beta - B)}\eta \\ \theta_t &= \theta_{t-1} + \epsilon g_{t-1} \mathbf{p}_{t-1} \end{aligned} \right\} \text{SGHMC Updates}$$

where $\eta \sim \mathcal{N}(\mathbf{0}, \mathbf{I})$ and ϵ is the step size. Chen et al. (2016) shows that the continuous-time dynamics of the above transitions can indeed preserve the stationary distribution $\pi(\theta) \propto \exp(-U(\theta))$. In practice, the update equation of the preconditioning SGHMC Eq. 13 is closely related to Adam optimizer as discussed in (Chen et al., 2016). Intuitively, this can

be regarded as a specially designed Adam with properly scaled Gaussian noise. Algorithm 4 shows the procedure of the partial amortized inference.

Algorithm 4: Amortized Inference + SGHMC

input: Data \mathbf{X}_O , step size ϵ , friction β , thinning τ , learning rate γ , initialized θ , max sample size N

Result: Variational parameter ϕ and $\{\theta_n\}_{n=1}^N$

Model and sampler initialization;

counter=0;

while *not converged* **do**

Sample minibatch $\mathbf{X}_S \in \mathbf{X}_O$;

Random masking with mask \mathbf{m} : $\tilde{\mathbf{X}}_S = \mathbf{X}_S \times \mathbf{m}$;

/* Inference Network Update */

Compute $\mathcal{L}(\tilde{\mathbf{X}}_S; \phi)$ using Eq.4;

q_ϕ : Optimize($\mathcal{L}(\tilde{\mathbf{X}}_S; \phi)$;Adam; γ);

/* SGHMC step */

Compute $\tilde{U}(\theta)$ using Eq.3 with proper scale;

θ : Simulate dynamics Eq.13;

/* Update the sample pool */

if counter= $K\tau$, where K is any positive integer **then**

| $\{\theta_n\} = \text{Update}(\{\theta_n\}, \theta, N)$; // Using FIFO procedure

end

counter+=1;

end

Appendix B. Conditional BELGAM

We follow the similar notations as in main text, but we have additional target sets \mathbf{Y}_O and \mathbf{Y}^* in observed training and test data respectively. By similar derivations in (Sohn et al., 2015), we have

$$\log p(\mathbf{Y}_O | \mathbf{X}_O, \theta) \geq \sum_{i \in \mathbf{X}_O} \left[\mathbb{E}_{q_\phi(\mathbf{z}_i | \mathbf{x}_i, y_i)} [\log p(y_i | \mathbf{z}_i, \theta)] - KL[q_\phi(\mathbf{z}_i | \mathbf{x}_i, y_i) || p(\mathbf{z}_i | \mathbf{x}_i)] \right] \quad (14)$$

Note that the encoder proposed in *BELGAM* can handle variable-sized inputs, thus, we can make further approximation $p(\mathbf{z}_i | \mathbf{x}_i) \approx q_\phi(\mathbf{z}_i | \mathbf{x}_i)$. We call the right hand side of Eq. 14 as $\mathcal{L}_{\text{conditional}}(\mathbf{Y}_O; \phi)$. We should note that $\mathcal{L}_{\text{conditional}}(\mathbf{Y}_O; \phi)$ only focuses on prediction quality. On the contrary, successful active prediction, as discussed in main text, requires the model not only has a better target prediction but also capture the correlations between input features for sequential active decisions. Thus, in practice, we need to include the Eq. 2 as well. Thus during each SGHMC step, Eq. 2 is replaced with

$$\mathcal{L}(\{\mathbf{Y}_O, \mathbf{X}_O\}; \phi) = \beta \mathcal{L}_{\text{conditional}}(\mathbf{Y}_O; \phi) + (1 - \beta) \mathcal{L}_{\text{joint}}(\mathbf{X}_O; \phi) \quad (15)$$

where β controls which tasks the model focuses on. When $\beta = 0.5$, we have

$$\log p(\{\mathbf{X}_O, \mathbf{Y}_O\}, \theta) \geq \mathcal{L}(\{\mathbf{X}_O, \mathbf{Y}_O\}; \theta) \quad (16)$$

with equality holds when $q_\phi(\mathbf{z}_i|\mathbf{x}_i) = p(\mathbf{z}_i|\mathbf{x}_i)$ and $q_\phi(\mathbf{z}_i|\mathbf{x}_i, y_i) = p(\mathbf{z}_i|\mathbf{x}_i, y_i)$. In experiment, we choose $\beta = 0.6$. We can also derive the equivalent form for Eq.4 using similar procedures for inference network update.

Appendix C. Information acquisition

C.1 Theoretical results

Review: EDDI. For the active target prediction, model need to decide which feature should be queried for the purpose of predicting the target \mathbf{Y} accurately in each test selection step. Ma et al. (2019) proposes a reward function for this test task inspired by Bayesian experimental design (Lindley, 1956; Bernardo, 1979). They propose to select the data point $x_{i,d}$ by maximizing:

$$R(x_{i,d}, \mathbf{X}_O) = \mathbb{E}_{x_{i,d} \sim p(x_{i,d}|\mathbf{X}_O)} [KL[p(\mathbf{y}_i|x_{i,d}, \mathbf{X}_O)||p(\mathbf{y}_i|\mathbf{X}_O)]]. \quad (17)$$

We find that this can be written as the mutual information between the target \mathbf{y}_i and the candidate $x_{i,d}$:

$$R(x_{i,d}, \mathbf{X}_O) = H[p(\mathbf{y}_i|\mathbf{X}_O)] - \mathbb{E}_{p(x_{i,d}|\mathbf{X}_O)} [H[p(\mathbf{y}_i|\mathbf{X}_O, x_{i,d})]]. \quad (18)$$

Thus, maximizing this quantity is equivalent to finding the most informative feature to the predictive target variable \mathbf{y}_i . However, this is not a suitable acquisition function in the training time as it is built on the assumption that the model is well trained and able to find the true informative features. Specifically, from Eq.18, it should be noted that $x_{i,d}$ is irrelevant to the first term. Thus, maximizing this objective is equivalent to minimizing the expected entropy after observing $x_{i,d}$, or conditional entropy $H(\mathbf{y}_i|x_{i,d})$. This objective purely encourages exploitation. For example, it can fail in the following scenario. In the beginning of training acquisition, the model may capture the wrong informative feature due to the small training data set. The exploitation nature of EDDI tends to pick this wrong feature over others in the following acquisitions and will be trapped into the sub-optimal strategy.

EDDI for PA-BELGAM. Next, we show that with a trained *PA-BELGAM*, the above objective can be approximated efficiently. We assume the decoupled posterior $p(\theta, \mathbf{Z}|\mathbf{X}_O) \approx p(\theta|\mathbf{X}_O)p(\mathbf{Z}|\mathbf{X}_O)$ and conditionally independent features $p(\mathbf{x}_i|\mathbf{z}_i, \theta) = \prod_{d=1}^{|\mathbf{o}_i|} p(x_{i,d}|\theta, \mathbf{z}_i)$. The EDDI rewards in Eq.17 can be rewritten by using KL chain rule:

$$\begin{aligned} KL[p(\mathbf{y}_i|x_{i,d}, \mathbf{X}_O)||p(\mathbf{y}_i|\mathbf{X}_O)] &= KL[p(\mathbf{y}_i, \mathbf{z}_i, \theta|x_{i,d}, \mathbf{X}_O)||p(\mathbf{y}_i, \mathbf{z}_i, \theta|\mathbf{X}_O)] \\ &\quad - \mathbb{E}_{p(\mathbf{y}_i|x_{i,d}, \mathbf{X}_O)} [KL[p(\mathbf{z}_i, \theta|\mathbf{y}_i, x_{i,d}, \mathbf{X}_O)||p(\mathbf{z}_i, \theta|\mathbf{y}_i, \mathbf{X}_O)]]. \end{aligned} \quad (19)$$

The first term can be further approximated as

$$\begin{aligned} KL[p(\mathbf{y}_i, \mathbf{z}_i, \theta|x_{i,d}, \mathbf{X}_O)||p(\mathbf{y}_i, \mathbf{z}_i, \theta|\mathbf{X}_O)] &= KL[p(\mathbf{z}_i, \theta|x_{i,d}, \mathbf{X}_O)||p(\mathbf{z}_i, \theta|\mathbf{X}_O)] \\ &\quad + KL[p(\mathbf{y}_i|\mathbf{z}_i, \theta, x_{i,d}, \mathbf{X}_O)||p(\mathbf{y}_i|\mathbf{z}_i, \theta, \mathbf{X}_O)] \\ &= KL[p(\mathbf{z}_i|x_{i,d}, \mathbf{X}_O, \theta)||p(\mathbf{z}_i|\mathbf{X}_O, \theta)] + KL[p(\theta|x_{i,d}, \mathbf{X}_O)||p(\theta|\mathbf{X}_O)] + KL[p(\mathbf{y}_i|\mathbf{z}_i, \theta)||p(\mathbf{y}_i|\mathbf{z}_i, \theta)] \\ &= KL[p(\mathbf{z}_i|x_{i,d}, \mathbf{X}_O)||p(\mathbf{z}_i|\mathbf{X}_O)]. \end{aligned} \quad (20)$$

where the last equality holds if we assume no posterior updates for θ . This is a reasonable assumption because $x_{i,d}$ is only single data point adding into a much larger set \mathbf{X}_O . By using similar trick, we can show the second term in Eq.19 is re-written as

$$\begin{aligned}
& \mathbb{E}_{p(\mathbf{y}_i|x_{i,d},\mathbf{X}_O)}[KL[p(\mathbf{z}_i, \theta|\mathbf{y}_i, x_{i,d}, \mathbf{X}_O)||p(\mathbf{z}_i, \theta|\mathbf{y}_i, \mathbf{X}_O)]] \\
&= \mathbb{E}_{p(\mathbf{y}_i|x_{i,d},\mathbf{X}_O)}[KL[p(\mathbf{z}_i|\mathbf{y}_i, x_{i,d}, \mathbf{X}_O)||p(\mathbf{z}_i|\mathbf{X}_O, \mathbf{y}_i)] + KL[p(\theta|\mathbf{y}_i, \mathbf{X}_O, x_{i,d})||p(\theta|\mathbf{X}_O, \mathbf{y}_i)]] \\
&= \mathbb{E}_{p(\mathbf{y}_i|x_{i,d},\mathbf{X}_O)}[KL[p(\mathbf{z}_i|\mathbf{y}_i, x_{i,d}, \mathbf{X}_O)||p(\mathbf{z}_i|\mathbf{X}_O, \mathbf{y}_i)]].
\end{aligned} \tag{21}$$

Then, we replace the posterior of \mathbf{Z} with variational approximations q_ϕ . Eq.17 can be approximated as

$$\begin{aligned}
R(x_{i,d}, \mathbf{X}_O) &\approx \mathbb{E}_{p(x_{i,d}|\mathbf{X}_O)}[KL[q_\phi(\mathbf{z}_i|x_{i,d}, \mathbf{X}_O)||q_\phi(\mathbf{z}_i|\mathbf{X}_O)]] \\
&\quad - \mathbb{E}_{p(x_{i,d},\mathbf{y}_i|\mathbf{X}_O)}[KL[q_\phi(\mathbf{z}_i|\mathbf{y}_i, x_{i,d}, \mathbf{X}_O)||q_\phi(\mathbf{z}_i|\mathbf{X}_O, \mathbf{y}_i)]].
\end{aligned} \tag{22}$$

This is exactly equivalent to the original form in (Ma et al., 2019). The only difference is the sampling stage for $x_{i,d} \sim p(x_{i,d}|\mathbf{X}_O)$ and $x_{i,d}, \mathbf{y}_i \sim p(x_{i,d}, \mathbf{y}_i|\mathbf{X}_O)$, where the θ samples are needed.

$$\begin{aligned}
& \mathbf{z}_i \sim q_\phi(\mathbf{z}_i|\mathbf{X}_O) \\
& \theta \sim p(\theta|\mathbf{X}_O) \quad \text{using SGHMC} \\
& x_{i,d} \sim p(x_{i,d}|\mathbf{z}_i, \theta) \\
& \mathbf{y}_i \sim p(\mathbf{y}_i|\mathbf{z}_i, \theta)
\end{aligned} \tag{23}$$

Connections of Icebreaker acquisition function to mutual information We now show that the information acquisition function proposed in Eq.10 with $\alpha = \frac{1}{2}$ is equivalent to the mutual information between θ and the feature-target pair $(\mathbf{y}_i, x_{i,d})$.

$$\begin{aligned}
R_c(x_{i,d}, \mathbf{X}_O) &= \underbrace{\frac{1}{2}H[p(x_{i,d}|\mathbf{X}_O)] + \frac{1}{2}\mathbb{E}_{p(x_{i,d}|\mathbf{X}_O)}[H[p(\mathbf{y}_i|x_{i,d}, \mathbf{X}_O)]]}_{\textcircled{1}} \\
&\quad - \underbrace{\frac{1}{2}\mathbb{E}_{p(\theta|\mathbf{X}_O)}[H[p(x_{i,d}|\theta, \mathbf{X}_O)]] - \frac{1}{2}\mathbb{E}_{p(\theta,x_{i,d}|\mathbf{X}_O)}[H[p(\mathbf{y}_i|\theta, x_{i,d}, \mathbf{X}_O)]]}_{\textcircled{2}}.
\end{aligned} \tag{24}$$

For $\textcircled{1}$, we have

$$\begin{aligned}
\textcircled{1} &= - \int p(x_{i,d}|\mathbf{X}_O) \left[\log p(x_{i,d}|\mathbf{X}_O) + \int p(\mathbf{y}_i|x_{i,d}, \mathbf{X}_O) \log p(\mathbf{y}_i|x_{i,d}, \mathbf{X}_O) d\mathbf{y}_i \right] dx_{i,d} \\
&= - \int p(x_{i,d}|\mathbf{X}_O) \int p(\mathbf{y}_i|x_{i,d}, \mathbf{X}_O) \log p(x_{i,d}, \mathbf{y}_i|\mathbf{X}_O) d\mathbf{y}_i dx_{i,d} \\
&= H[p(\mathbf{y}_i, x_{i,d}|\mathbf{X}_O)].
\end{aligned} \tag{25}$$

For ②:

$$\begin{aligned}
\textcircled{2} &= \int p(\theta, x_{i,d} | \mathbf{X}_O) \left[\log p(x_{i,d} | \theta, \mathbf{X}_O) + \int p(\mathbf{y}_i | \theta, x_{i,d}, \mathbf{X}_O) \log p(\mathbf{y}_i | \theta, x_{i,d}, \mathbf{X}_O) d\mathbf{y}_i \right] d\theta dx_{i,d} \\
&= \int p(\theta, x_{i,d} | \mathbf{X}_O) \left[\int p(\mathbf{y}_i | \theta, x_{i,d}, \mathbf{X}_O) \log p(\mathbf{y}_i, x_{i,d} | \theta, \mathbf{X}_O) d\mathbf{y}_i \right] d\theta dx_{i,d} \\
&= \int p(\mathbf{y}_i, x_{i,d}, \theta | \mathbf{X}_O) \log p(\mathbf{y}_i, x_{i,d} | \theta, \mathbf{X}_O) d\mathbf{y}_i dx_{i,d} d\theta \\
&= -\mathbb{E}_{p(\theta | \mathbf{X}_O)} [H[p(\mathbf{y}_i, x_{i,d} | \theta, \mathbf{X}_O)]] .
\end{aligned} \tag{26}$$

Thus, the Eq.10 with $\alpha = \frac{1}{2}$ is written as

$$R_C(x_{i,d}, \mathbf{X}_O) = \frac{1}{2} (H[p(\mathbf{y}_i, x_{i,d} | \mathbf{X}_O)] - \mathbb{E}_{p(\theta | \mathbf{X}_O)} [H[p(\mathbf{y}_i, x_{i,d} | \theta, \mathbf{X}_O)]]) = \frac{1}{2} I(\theta, \{\mathbf{y}_i, x_{i,d}\} | \mathbf{X}_O) . \tag{27}$$

Appendix D. Training details

In this section, we give details about the experiment setup and the training acquisition.

D.1 Training time acquisition

We compute the Icebreaker acquisition functions (Eq.10 or Eq.5) for the entire pool set \mathbf{X}_U . During the selection, we apply two heuristics. First, instead of picking the top K values, we first normalize their rewards r_{id} with temperature T :

$$w_{id} = \frac{\exp(r_{id}/T)}{\sum_{r_{id}} \exp(r_{id}/T)} \tag{28}$$

Then, we sample $x_{i,d}$ according to their weights w_{id} . This is a common trick in the active learning techniques to encourage some exploration (Zhu and Bento, 2017; Baram et al., 2004). When $T \rightarrow 0$, this sampling becomes the maximization. The second heuristic is to balance the selected feature number from the observed and new instances. Specifically, assume we need to select K values from the pool, we use the above procedure to select $\frac{K}{2}$ from the rows that have been queried with at least one feature before and other $\frac{K}{2}$ from the rows that are completely new. This is to balance the proportion of exploiting the observed rows and exploring the new ones. For a fair comparison, the second heuristic is applied for all the baselines as well.

D.2 Training hyperparameters

UCI. We split the whole data set into the training and test sets with proportion 80% and 20%. In order to mimic that some features may not be available for query, we manually mask 20% in the training set. For the imputation task, 40% of the data in the test set are masked as the test target and the remaining 60% are reserved as the test input. For the active prediction, we only mask the target variable in the test set as the test target. We also

sample 2% of the data instance as the pre-train data as the model has not learned anything in the beginning and the acquisition is the same as random.

We use 5-dimensional latent variable \mathbf{z} and the embedding for each feature \mathbf{e}_d has 10 dimensions. $h(\cdot)$ is a neural network with 1 hidden layer of 20 units. The aggregation function $g(\cdot)$ is the summation. For the decoder, it has the structure $5 - 100 - 40 - X$, where X is the output dimensions. The data set is normalized with 0 mean and unit variance. We use $\alpha = 1$ and $\alpha = 0.4$ in Eq.10 for the imputation and the active prediction training time acquisition respectively. We use the learning rate 0.003 for the Adam optimizer and $\epsilon^2 = 0.0003$ for the SGHMC step size. We also use $\tau = 0.99$, and $\epsilon\beta = 0.1$ for the SGHMC hyperparameters. The model is trained with 1500 epochs and 100 mini-batch size. The first 750 epochs are used for the SGHMC burn-in and no θ samples are recorded. At each training time acquisition, the model selects 25 and 50 values from the pool for the active prediction and the imputation respectively.

MovieLens-1M. The *MovieLens-1m* data set contains 1 million ratings for 3000 movies from 6000 users. Each rating is a categorical data ranging from 1 to 5. We follow the same data pre-processing procedure as (Houlsby et al., 2014) by selecting 1000 movies and 2000 users with the highest number of ratings. We follow the same settings as the UCI imputation with 0.5% data as the pre-train and 20% of the values in the test set as the targets. The model picks 5000 data points from the pool at the training acquisition followed by a model re-initialization to avoid local optima (Gal et al., 2017).

The latent and feature embedding dimensions are 100 and 50 respectively. The decoder structure is the same as the UCI setting apart from the input and output dimensions. The learning rate and hyperparameters for Adam and SGHMC are the same as the UCI imputation. We train the model using 300 epochs with 100 batch size. Similarly we use half of the total epochs for the SGHMC burn-in. Each training acquisition selects 2000 values from the pool.

MIMIC III. The latent and feature embedding dimensions are the same as the UCI active prediction. The decoder structure is changed to $5 - 100 - 100 - 18$, where 18 is the data dimension of MIMIC III. The step size of SGHMC is changed to $\epsilon^2 = 0.0001$. The model is trained for 500 epochs with 100 batch size. The pre-train data set size is 0.5% of the pool data. Each training acquisition selects 50 values from the pool set. The data normalization is the same as the UCI.

D.2.1 MIMIC III DATA SET STATISTICS

MIMIC III data set after being processed by (Harutyunyan et al., 2017) is extremely imbalanced, where around 88% of the data has label 0. Thus, training with this data set will result in a lazy model that only outputs label 0. Typically additional pre-processing method for such data set is needed. In this project, we manually balance the data by taking an equal number of instances with label 0 and 1, which forms a new, balanced data set. We do the same for the test set as well. Figure 8 (Left) shows the feature label and its missing proportion in MIMIC III. Table 1 shows the acronym of each label. From Figure 8 (middle and right), we can observe there is a clear shift of importance for *Glucose*. We hypothesize the reason is that the relationship of *Glucose* and target is less linear and cannot be captured by the linear model. For the Icebreaker, when the training data set is small, it is easier to

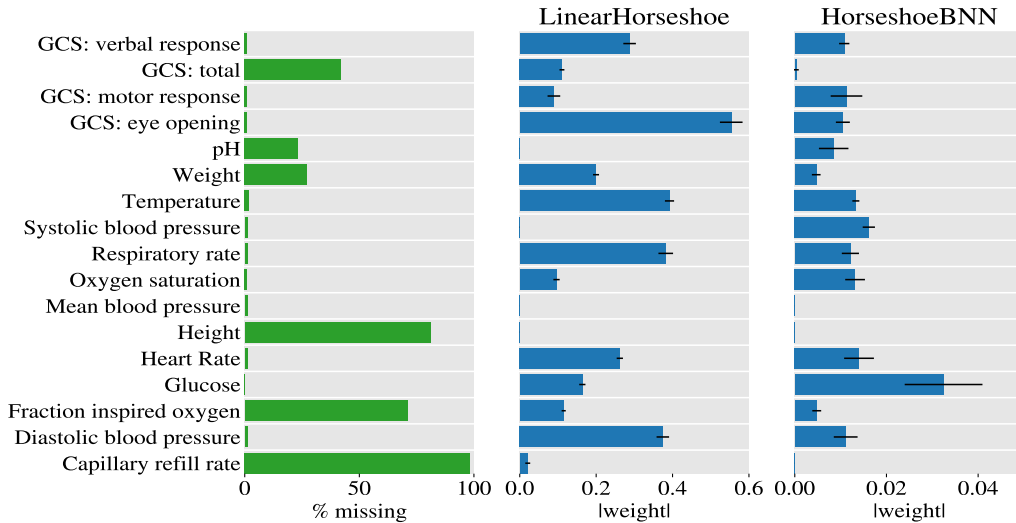


Figure 8: (Left) The missing proportion of each feature in MIMIC III. (Middle and Right) The norm of the weights. Zero feature weights indicate the corresponding feature is irrelevant to the target according to the model. This figure is directly taken from Popkes et al. (2019).

Acronym	Label	Abbrv.	Label
<i>Cap.</i>	Capillary refill rate	<i>Glu.</i>	Glucose
<i>Dia.BP</i>	Diastolic blood pressure	<i>HR</i>	Heart Rate
<i>Ins.Oxy</i>	Fraction inspired oxygen	<i>Hei.</i>	Height
<i>GCS:E</i>	GCS: eye opening	<i>MBP</i>	Mean blood pressure
<i>GCS:M</i>	GCS: motor response	<i>Oxy.Sat</i>	Oxygen saturation
<i>GCS:T</i>	GCS: total	<i>Res.R</i>	Respiratory rate
<i>GCS:V</i>	GCS: verbal response	<i>Temp</i>	Temperature
<i>Wei.</i>	Weight		

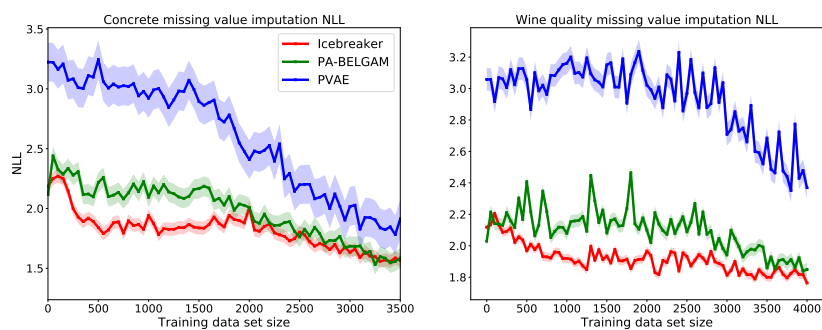
Table 1: Label and its Acronym

pick up simple relationships. Thus, *Glucose* seems to be less relevant in the beginning. But as the data set grows, Icebreaker can capture non-linear dependencies and start to value the importance of *Glucose*.

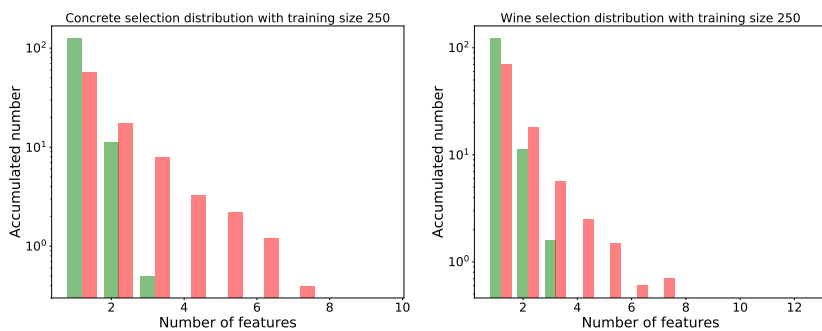
Appendix E. Additional UCI Results

For imputation task, we also evaluate the performance of Icebreaker on *Concrete* and *Wine quality* data sets. For the active prediction, we investigate its performance and feature selection strategy in a simple data set called *Energy*. For all these experiments, we follow the experiment setup mentioned previously.

Imputation. Figure 9a shows the imputation NLL curve as the data set grows. As expected, Icebreaker outperforms the baselines, especially when the training data size is



(a) NLL Curve



(b) Long Tail Selection

Figure 9

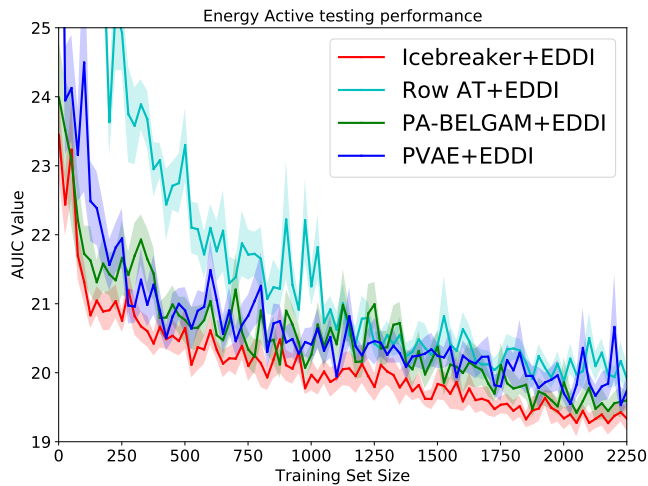


Figure 10: AUIC curve w.r.t. *Energy* data set size

small. Figure 9b shows the selection pattern of Icebreaker, where we can observe a long-tailed strategy similar to *Boston housing* and *MovieLens-1m* imputation.

Active Prediction. Figure 10 shows the AUIC curve as training data set size grows. We can see Icebreaker still outperforms the other 3 baselines by a small margin. The possible

reason is that the *Energy* data set is a very simple data set with clear informative variables. We choose this set for the purpose of diagnosing the selection strategy of Icebreaker rather than achieving significant improvement over others. To investigate the strategy of Icebreaker, we group the features in *Energy* data set into 4 groups: *Useful for target*, *Useful*, *Harder to learn* and *Useless* based on the middle panel in Figure 11.

The x-axis in the middle panel of Figure 11 represents the sorted target value from low to high. Y-axis indicates the feature values corresponding to the target. We can see for the *blue* line, it has a clear boundary at target value -0.3 and the oscillation of this line is not large compared to others. Thus, it acts as an indicator feature to separate the small and large target values, which is the most useful one for predicting target. As for the *red* curve, it still has a relatively clear boundary but the large oscillation indicates this is not a robust feature for the prediction. So we refer to it as "*Useful*". Similar for *green* curve, its boundary is less clear and it has a even larger oscillation. Therefore, we call it "*harder to learn*". As for the black curve, it acts as the pure noise and has no clear correlations to target variables. We classify this as "*Useless*" features.

From the left panel in Figure 11, initially, "*Harder to Learn*" and "*Useless*" features are selected the most. This is because the objective Eq.10 encourages the model to find the informative but hard features. Due to the initially scarce training data, the model successfully figures out they are hard to learn but fails to identify which one is more informative. Thus, the selected elements for both features increases in a similar trend. With the data set growing, the model finds out the useless feature. Although it is hard to learn, the model still reduces its query frequency. As for the other two useful features, the model starts to select more of them after 800 data points.

The right panel in Figure 11 shows the initial choice made by the model during the active prediction. There are actually two features that can be classified as '*Useful for target*'. But we only plot one of them in the left and middle panel of Figure 11 for clarity. The other one is plotted in the right panel of Figure 11 with light *blue*. It is the same for '*Useful*' features.

It is expected that the '*Useful for target*' feature is regarded as the most important one by the model though they are not selected the most in training. '*Useful*' and '*Harder to Learn*' features are also selected with the number decreasing according to their importance. As expected, the '*Useless*' features are not selected at all. Thus, the Icebreaker can indeed discover the important features and select the hard ones among them.

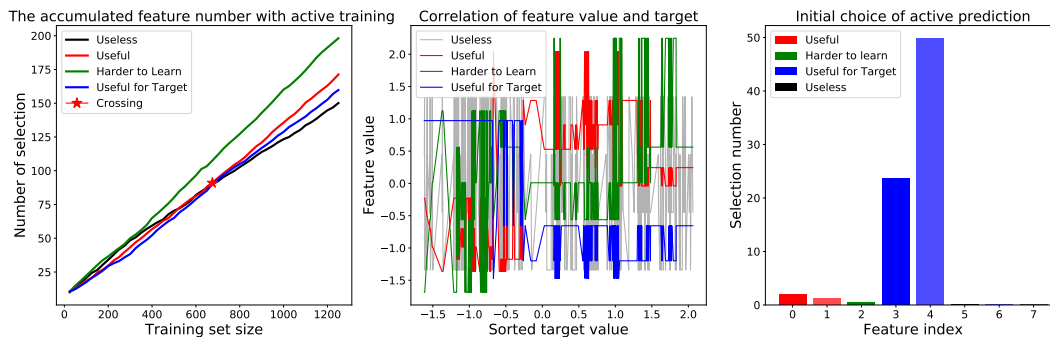


Figure 11: (Left) Accumulated feature number (Middle) Correlations between the features and target (Right) Initial choice at the test time acquisition.